Applied Chemical Engineering (2023) Volume 7 Issue 1
doi: 10.24294/ace.v7i1.2258

ORIGINAL RESEARCH ARTICLE

Thermal degradation of 3D printing processed polylactide samples by means of vibrational spectroscopy

P. Siafarika[1], D.E. Mouzakis[2], N.K. Nasikas[2,*], A.G. Kalampounias[1,3,*]

[1] *Department of Chemistry, University of Ioannina, GR-45110 Ioannina, Greece*

[2] *Department of Military Sciences, Division of Mathematics and Engineering Sciences, Hellenic Army Academy, GR-16673 Vari, Greece*

[3] *University Research Center of Ioannina (URCI), Institute of Materials Science and Computing, GR-45110 Ioannina, Greece*

*** Corresponding authors:** N.K. Nasikas, nasikas@sse.gr; A.G. Kalampounias, akalamp@uoi.gr

ABSTRACT

In the present study, we utilized the fused deposition modeling technique (FDM) to prepare polylactide (PLA) samples and evaluate in real time their thermal degradation by means of vibrational spectroscopy. The FDM method is probably the most popular technology among 3D printing technologies due to the inexpensive and flexible extrusion systems used for the handling of several thermoplastic materials. Nevertheless, a thermal degradation phenomenon of the 3D-printed thermoplastic PLA samples occurs, which is an inevitable issue for long-term reliability of the material leading to poor product properties. We recorded the Fourier transform infrared spectra in real-time mode to monitor the thermal degradation kinetics of PLA samples at a specific temperature below the glass transition point and explore the induced structural alterations. The absorbance of specific spectral features was used to evaluate the concentration reduction of PLA functional groups during the thermal degradation process. The kinetics of the thermal degradation was estimated by means of the absorbance of the C-COO band which reflects the scission of the ester linkage due to degradation process. The kinetic rate constant was found $K_t = 2.30 \times 10^{-3}$ s^{-1}. The results reported in this work were analyzed and discussed in view of relevant data reported for PLA samples prepared with traditional mechanical processing.

Keywords: polylactide; FTIR spectroscopy; degradation kinetics; real-time monitoring; 3D printing

ARTICLE INFO

Received: 15 June 2023
Accepted: 24 August 2023
Available online: 29 December 2023

1. Introduction

Polylactic acid or polylactide (PLA) is a thermoplastic polyester with a molecular backbone formula of $(C_3H_4O_2)_n$. This polyester can be received by condensation of lactic acid after a loss of water. Alternatively, it can be formed by ring-opening polymerization of lactide, which is the cyclic dimer of the basic repeating unit of the polymer. PLA may exist in several distinct forms due to the inherent chiral nature of the lactic acid. Several physical properties, such as the degree of crystallinity, are strongly affected and to a large extent controlled by the ratio of D-to-L enantiomers used for the final product. In this procedure, the type of the catalyst used is also a controlling factor, although to a much lesser extent[1]. Despite the fact that the name polylactic acid is extensively used, this name is potentially ambiguous or confusing since it does not comply with the standard IUPAC nomenclature, which is poly(lactic acid). Nevertheless, the name polylactic acid is used since PLA is not a polyacid (polyelectrolyte), but a polyester[2]. It can be dissolved in

dichloromethane, while acetone softens its surface, making it sticky without any dissolution, and can be used for welding to another PLA surface[2]. PLA has become a popular material since it is a biodegradable polymer that is being economically produced from renewable resources[3]. Its widespread application has been hindered by numerous physical and processing shortcomings, such as the hasty loss of molecular weight during the melting process[4].

PLA is the one of the most widely used plastic filament material not only for 3D printing purposes, but also for applications such as casting, injection moulding, extrusion, machining, and solvent welding[5,6]. Due to its attractive physical properties including low melting point, high strength, low thermal expansion, good layer adhesion, and high heat resistance when annealed, PLA is an ideal material for these applications. Furthermore, PLA has the lowest heat resistance of the common 3D printing plastics even without annealing[7]. PLA has also been used in biomedical applications[8,9], agricultural[10] and packaging[11]. Concerning biomedical applications, PLA is suitable for use as medical implant in the form of anchors, screws, plates, pins, rods, mesh and as a polymeric scaffold for drug delivery purposes[12].

Degradation of PLA occurs by the so-called Amycolatopsis and Saccharothrix bacteria, and by several enzymes, such as pronase and proteinase K[13]. PLA may also be degraded abiotically by three main mechanisms[14]. These mechanisms include (i) hydrolysis, where the ester groups of the main chain are cleaved causing reduction of the molecular weight, (ii) thermal decomposition, which leads to the appearance of different compounds such as lighter molecules and linear and cyclic oligomers with different molecular weight and lactide, and (iii) photodegradation, where UV radiation induces degradation. In the presence of moisture during melt processing, such as at the 3D printer nozzle, the degradation process called “thermohydrolysis” may occur. In our case, special attention has been paid to minimize atmospheric humidity by controlling the sample inert atmosphere.

Vibrational spectroscopy may provide an effective tool for real time monitoring of the evolution of PLA degradation and bridges the gap between sample collection and characterization[15]. The sampling is fast and permits characterization of polymer thermal degradation by analyzing the spectral changes in chemical bonds participating in specific functional groups that are strongly affected by degradation and provide kinetic information[16].

The aim of the present work is to study the thermal degradation kinetics of PLA samples fabricated by 3D printing by means of Fourier transform infrared spectroscopy. The thermal degradation was investigated at a fixed temperature near glass transition temperature as a function of residence time. The effect was explored in detail by measuring in real-time the absorbance of specific bands attributed to functional groups that are strongly influenced by the degradation process. Thermal degradation kinetics can help in understanding the degradation mechanisms and analyze the thermal degradation process. In-situ high-temperature Raman spectroscopy is an effective technique to assess the thermal degradation kinetics of polymeric materials.

2. Experimental

2.1. Materials

Polylactic acid with a density of 1.21 g/cm^3 was purchased from Neema3D (NL) batch 15058907.

PLA was first dried below glass transition point at 60 °C in an oven for several hours to remove any adsorbed moisture before extrusion procedure.

All PLA specimens in the form of circular disks, were designed by using CAD software (FreeCAD), and exported in STL file format (3D Systems), to CURA (Ultimaker) software. Afterwards, the specimen designs were digitally sliced by CURA, having incorporated the required printing parameters. The specimens were 3D printed using a Fused Deposition Modeling (FDM) 3D printer (Creality CR-200B, Shenzhen Creality 3D

Technology Co., Ltd., Shenzhen, China) with the following parameters. The nozzle diameter was 0.4 mm, the temperature of the nozzle was set at 225 °C with a raster angle of 0°, the bed temperature was kept at 60 °C. The thickness of the layer and the infill density were fixed at 0.2 mm and 100%, respectively. The CR-200B is a fully enclosed 3D printer system so, isothermal printing conditions were ensured. The final specimen thickness achieved was $t = 2 \pm 0.2$ mm.

The so-obtained PLA samples, were cooled to room temperature and collected for the characterization and thermal degradation analysis.

2.2. Fourier transform infrared spectroscopy

All mid-infrared spectra were recorded in the 4000 to 370 cm^{-1} spectral region from KBr pellets under isobaric conditions with a compact FT/IR-4700 spectrometer by Jasco in transmittance mode. Spectroscopic grade potassium bromide powder was used to prepare mixtures with a mixing ratio 4 mg of PLA sample/100 mg of dry KBr, and afterward pressed into pellets with a thickness of ~1 mm. The spectrometer was equipped with a stable 45° Michelson sealed interferometer with corner-cube mirror, auto-alignment, and DSP control. For all spectroscopic measurements the spectral resolution was set at 2 cm^{-1}. The signal-to-noise ratio was 35,000:1. The FTIR spectrometer has sealed and desiccated optics and utilizes a DLATGS detector with Peltier temperature control. The light source was a standard high-intensity ceramic source. The spectrum of an "empty" KBr pellet was recorded prior to each FTIR measurement as a background to account for atmospheric vapor compensation and KBr absorption.

The PLA samples were heated at 60 °C and remained there for several residence times allowing real time monitoring of the thermal degradation utilizing the FTIR600 heating stage by Linkam. The FTIR600 stage allows infrared analysis of samples from −195 °C up to 600 °C under environmental control. The temperature controller of the FTIR600 hot stage, optimized for FTIR systems, was able to maintain the temperature during each measurement fixed, with stability better than 0.1 °C. The FTIR600 stage was mounted vertically inside the cabinet of the spectrometer setup. The silver block of FTIR600 has a tapered hole and barium fluoride optical windows to allow maximum transmittance of IR without interference. A short review of the experimental protocols can be found elsewhere[17–19]. A schematic representation of the sample form and of the heating equipment used for recording the high-temperature spectra as a function of time is presented in **Scheme 1**.

FTIR transmittance measurements were performed at 60 °C every 10 min up to 2 h and then every 60 min up to 8 h.

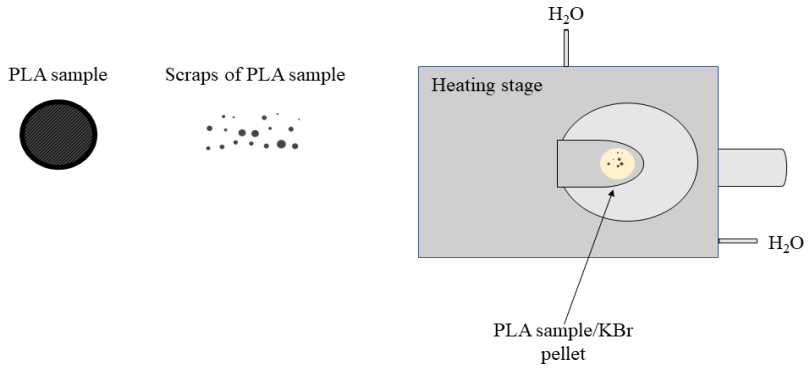

Scheme 1. A schematic representation of the sample form and heating equipment used for recording the high-temperature spectra as a function of time.

3. Results and discussion

3.1. Spectral sensing of PLA thermal degradation

The FT-IR spectra of PLA and lactic acid monomer are demonstrated in **Figure 1**. Both spectra are characterized by several peaks that are attributed to the stretching and bending vibrations of common functional groups. The chemical structure of monomeric and polymeric species is also shown.

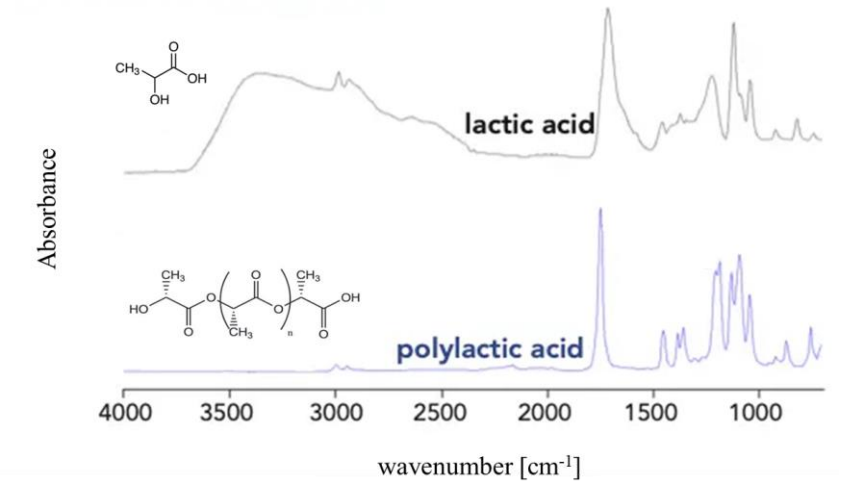

Figure 1. FTIR absorbance spectra of lactic (top) and polylactic (bottom) acid recorded under ambient conditions. The chemical structure of monomeric and polymeric species is also shown. See text for details concerning spectral conditions.

As it is expected, there exist several spectral similarities between the spectra of monomer and polymer. In brief, some of the main characteristic absorption bands of PLA are observed ~1757 cm^{-1} which ascribed to the stretching vibration of the C=O groups, ~1688 cm^{-1} that is related with the cis-elimination reaction leading to the formation of molecules with acrylic end groups containing C=C and at ~1450 cm^{-1} which is attributed to the C-H bending vibrations of the CH_3 functional groups[20,21]. Furthermore, the bands shown in the spectra at ~1126 and 1041 correspond to the CH_3 rocking vibration and C-CH_3 stretching vibration, respectively. Additionally, the peak at ~868 cm^{-1} is associated with the C-COO stretching vibration[20,21]. The frequencies of these bands and their assignment is summarized in **Table 1**.

Table 1. Main characteristic FTIR bands of PLA in wavenumbers and their assignment. These vibrational modes are affected by the degradation process.

Wavenumber [cm^{-1}]	**Band assignment**
868	C-COO stretching mode
1041	C-CH_3 stretching mode
1126	CH_3 rocking
1450	CH_3 bending mode
1688	C=C stretching mode
1757	C=O stretching mode

Figure 2 illustrates representative FTIR absorbance spectra of PLA during thermal degradation at 60 °C. Inside plot, the dashed and solid frames denote the characteristic bands where the analysis of the degradation process is focused. The absorbance of these bands is strongly affected by the degradation process and the integrated areas of the absorbance peaks can be used to quantitatively follow the progress of the degradation process as a function of time.

Figure 3a,b display the time evolution of the relative FTIR absorbance of the characteristic bands located

at 868 and 1041 cm^{-1}, respectively. We will focus our attention to the absorbance of the characteristic band at 868 cm^{-1} since this band is the most strongly affected from the thermal degradation of PLA which occurs at the ester linkage of the molecular chain. The lines observed in **Figure 3** correspond to a simple exponential decay that will be used to analyze the degradation kinetics in the next section.

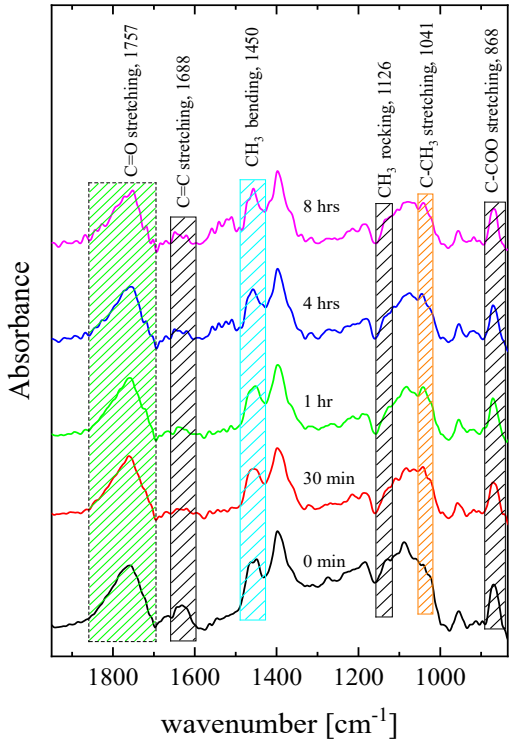

Figure 2. Representative normalized FTIR absorbance spectra of PLA during thermal degradation at 60 °C. The dashed and solid frames denote the characteristic bands where the analysis of the degradation process is focused. Numbers in parentheses denote vibrational frequencies in wavenumbers (cm^{-1}).

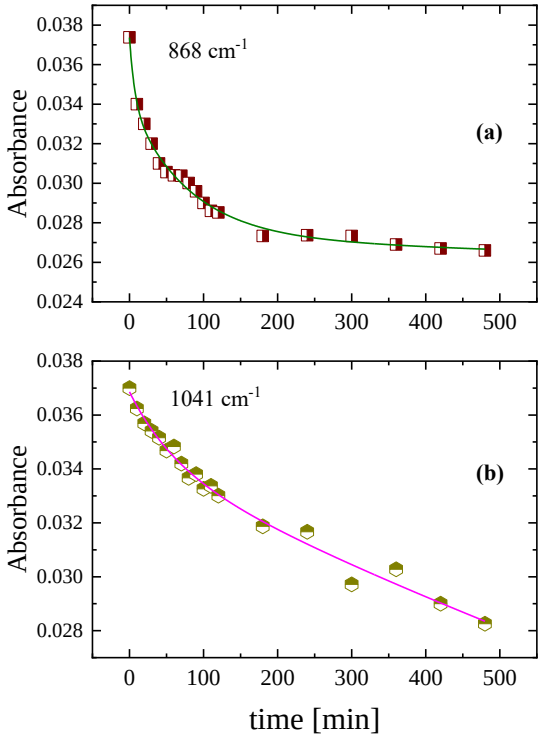

Figure 3. Time evolution of the relative FTIR absorbance of the characteristic bands located at **(a)** 868 and **(b)** 1041 cm^{-1}. Lines correspond to a simple exponential decay. See text for details concerning the fitting procedure.

In **Figures 4** and **5** is shown the time evolution of the relative FTIR absorbance of the characteristic bands located at 1126, 1450 cm^{-1} and 1688, 1757 cm^{-1}, respectively.

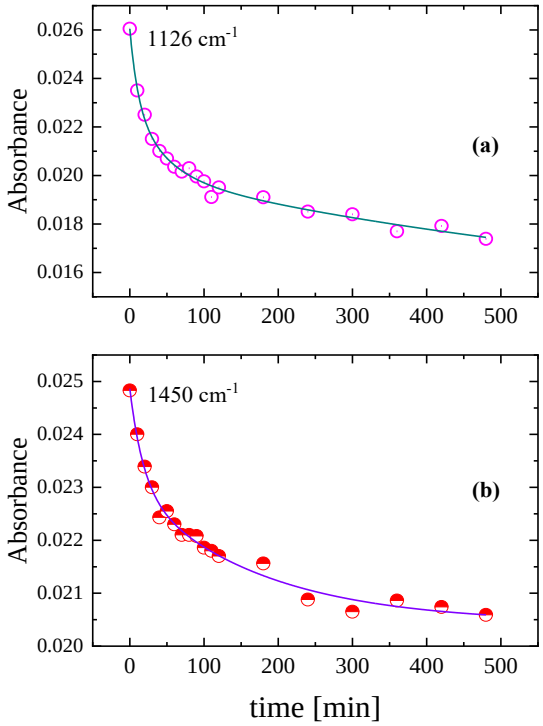

Figure 4. Time evolution of the relative FTIR absorbance of the characteristic bands located at **(a)** 1126 and **(b)** 1450 cm^{-1}. Lines are drawn as guide to the eye.

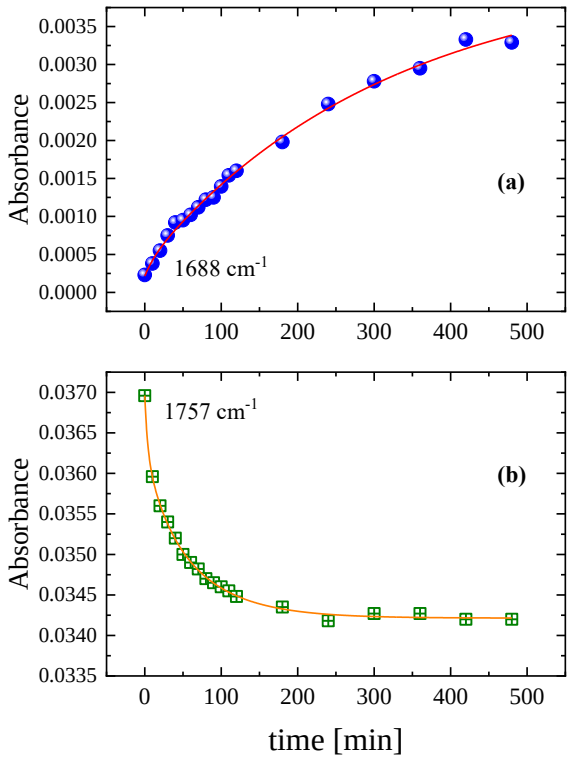

Figure 5. Time evolution of the relative FTIR absorbance of the characteristic bands located at **(a)** 1688 and **(b)** 1757 cm^{-1}. Lines are drawn as guide to the eye.

The bands at 868, 1126, and 1450 cm^{-1} are expected to diminish their absorbances due to the random chain scission and the intramolecular transesterification because of the induced thermal degradation process[22].

The absorbance of the 1757 cm^{-1} also exhibits the same behavior with a parallel frequency shift at higher frequencies indicating the hastening of the C=O stretching vibration. The absorbance decrease is attributed to the expanding depolymerization reaction that reduces the C=O content with a simultaneous formation of acetaldehyde[23]. It is interesting to note that the only case where the absorbance increases with increasing degradation time is the 1688 cm^{-1} band due to the formation of molecules with acrylic end groups containing C=C. Furthermore, the absorbances of almost all bands reveal a relatively sudden drop for the first 30 minutes and then tend to level off. The overall trend of the FTIR spectra degradation time is similar to that observed in molten polylactide by means of Raman spectroscopy[16]. According to previous studies, the volatile gaseous products generated from the thermal degradation of PLA predominantly contains lactide, cyclic oligomers, acetaldehyde, carbon dioxide, carbon monoxide, and methylketene (see e.g., Ref. 12). Thus, it is not so safe based on the experimental findings of the present work, to provide a frank description of the "new" chemical products from the thermal degradation process and the relevant chemical reactions.

3.2. Thermal degradation kinetics

The kinetic of the thermal degradation process in PLA can be monitored through the absorbance variation of the 868 cm^{-1} characteristic band, which is related with the ester linkage of the molecular chain. The scission of the ester linkage is assumed as first order reaction[24]. The equation which provides the variation rate of the ester concentration C_{ester} is:

$$\frac{dC_{ester}}{dt} = -K_t C_{ester} \tag{1}$$

with K_t denoting the degradation rate constant. Solving the above equation, we obtain:

$$C_{ester} = e^{-K_t t} + c_0 \tag{2}$$

where c_0 representing the integration constant.

The absorbance A of the 868 cm^{-1} band is related with the ester concentration C_{ester} through the Beer-Lambert law:

$$A = \varepsilon d C_{ester} \tag{3}$$

Parameter ε and d represent the molar absorptivity and the optical path length, respectively.

By combining Equations (2) and (3), we receive the ester linkage absorbance as a function of degradation time:

$$A(t) = \varepsilon d e^{-K_t t} + c_1 \tag{4}$$

with $c_1 = \varepsilon d c_0$. This equation was used to fit the time evolution of the FTIR absorbance of the characteristic band located at 868 cm^{-1}, which is presented in **Figure 3a**. The kinetic rate constant was found $K_t = 2.30 \times 10^{-3}$ s^{-1} with $R^2 = 0.99342$ revealing that the fitting model is adequate to describe the thermal degradation of PLA. The relevant kinetic rate constant for PLA melt at 220 °C under oxygen atmosphere was reported equal to $K_t = 1.31 \times 10^{-3}$ s^{-1}[16]. This difference can be understood considering that our working temperature is 60 °C that is below the glass transition temperature and far away from the 220 °C which is above melting point (T_m ~180 °C). Furthermore, our sample was prepared by utilizing a 3D printing technique. By differentiating the ester linkage absorbance, we calculate the change rate as a function of degradation time:

$$\left|\frac{dA}{dt}\right| = \left|\frac{dke^{-K_t t}}{dt}\right| = |c_2| e^{-K_t t} \tag{5}$$

with $c_2 = -K_t \varepsilon d$. Thermal degradation tests and the relevant kinetic analysis performed in this work established that the behavior of PLA samples differ depending on the procedures used to handle the initial material, namely traditional mechanical processing or 3D printing technology and further imply that there will be an effect on the mechanical properties of the PLA samples. It is reasonable to expect that the input parameters of the fused deposition process, including layer thickness, wall shell thickness, printing temperature,

infill structure, infill density percentage, and printing speeds, will have a strong impact on the mechanical proprieties of the printed final products. These parameters should be considered in order to be able to quickly generate complex structures with specific surface characteristics at the lowest possible cost and material losses for specific applications in sectors, such as the automotive, aerospace, medical, architecture, food, and arms industries.

4. Conclusions

The present study demonstrates the ability of vibrational spectroscopy and more specifically the Fourier transform infrared spectroscopy to monitor in real-time the thermal degradation of PLA samples prepared with 3D printing technique instead of traditional mechanical processing. FTIR transmittance spectra were recorded at 60 °C every 10 min up to 2 h and then every 60 min up to 8 h. The spectra revealed gradual variation as a function of degradation time. The absorbance of specific bands was used to quantitatively follow the smooth spectral variation with residence time at the specific temperature, which is close to the glass transition temperature of the material. These bands were strongly affected by the degradation process and can be used to monitor progress of the process as a function of time. Special attention has been paid on the 868 cm^{-1} band, which is attributed to the stretching mode of C-COO and it is the most strongly affected spectral feature from the thermal degradation of PLA which causes a scission of the ester linkage.

The absorbance of all bands revealed a relatively sudden drop for the first 30 min and then tended to level off. The kinetics of the PLA thermal degradation has also been evaluated and compared with relevant literature data of PLA samples prepared with conventional methods. The scission of the ester linkage was found to be a first order reaction as in the case of PLA samples prepared with traditional methods. The kinetic rate constant was found $K_t = 2.30 \times 10^{-3}$ s^{-1}. The results revealed that the degradation kinetics is slightly different and that the input parameters of the fused deposition process should be taken into account in order to be able to control the mechanical properties of the final product depending on the specific application.

Author contributions

Conceptualization, AGK and NKN; methodology, AGK; validation, PS, DEM, NKN and AGK; formal analysis, AGK, PS; investigation, PS, DEM, NKN and AGK; resources, DEM, NKN and AGK; data curation, PS, DEM, NKN and AGK; writing—original draft preparation, AGK; writing—review and editing, PS, DEM, NKN and AGK; supervision, AGK; project administration, NKN, AGK; funding acquisition, DEM, NKN and AGK. All authors have read and agreed to the published version of the manuscript.

Conflict of interest

The authors declare no conflict of interest.

References

1. Tsuji H, Ikada Y. Properties and morphologies of poly(l-lactide): 1. Annealing condition effects on properties and morphologies of poly(l-lactide). Polymer 1995; 36(14): 2709–2716. doi: 10.1016/0032-3861(95)93647-5
2. Martin O, Avérous L. Poly(lactic acid): Plasticization and properties of biodegradable multiphase systems. Polymer 2001; 42(14): 6209–6219. doi: 10.1016/S0032-3861(01)00086-6
3. Dash A, Kabra S, Misra S, et al. Comparative property analysis of fused filament fabrication PLA using fresh and recycled feedstocks. Materials Research Express 2022; 9(11): 115303. doi: 10.1088/2053-1591/ac96d4
4. Peelman N, Ragaert P, Ragaert K, et al. Heat resistance of biobased materials, evaluation and effect of processing techniques and additives. Polymer Engineering & Science 2018; 58(4): 513–520. doi: 10.1002/pen.24760
5. Lunt J. Large-scale production, properties and commercial applications of polylactic acid polymers. Polymer Degradation and Stability 1998; 59(1–3): 145–152. doi: 10.1016/S0141-3910(97)00148-1
6. Södergård A, Stolt M. Properties of lactic acid based polymers and their correlation with composition. Progress in Polymer Science 2002; 27(6): 1123–1163. doi: 10.1016/S0079-6700(02)00012-6

7. Xing R, Huang R, Qi W, et al. Three-dimensionally printed bioinspired superhydrophobic PLA membrane for oil-water separation. AIChE Journal 2018; 64(10): 3700–3708. doi: 10.1002/aic.16347
8. Middleton JC, Tipton AJ. Synthetic biodegradable polymers as orthopedic devices. Biomaterials 2000; 21(23): 2335–2346. doi: 10.1016/S0142-9612(00)00101-0
9. Saini P, Arora M, Ravi Kumar MNV. Poly(lactic acid) blends in biomedical applications. Advanced Drug Delivery Reviews 2016; 107: 47–59. doi: 10.1016/j.addr.2016.06.014
10. Rocha DB, Souza de Carvalho J, de Oliveira SA, dos Santos Rosa D. A new approach for flexible PBAT/PLA/$CaCO_3$ films into agriculture. Journal of Applied Polymer Science 2018; 135(35): 46660. doi: 10.1002/app.46660
11. Auras R, Harte B, Selke S. An Overview of polylactides as packaging materials. Macromolecular Bioscience 2004; 4(9): 835–864. doi: 10.1002/mabi.200400043
12. Auras R, Lim LT, Selke SEM, Tsuji H. Poly(Lactic Acid): Synthesis, Structures, Properties, Processing, and Applications. John Wiley & Sons; 2011.
13. Castro-Aguirre E, Iñiguez-Franco F, Samsudin H, et al. Poly(lactic acid)—Mass production, processing, industrial applications, and end of life. Advanced Drug Delivery Reviews 2016; 107: 333–366. doi: 10.1016/j.addr.2016.03.010
14. Tokiwa Y, Calabia BP, Ugwu CU, Aiba S. Biodegradability of plastics. International Journal of Molecular Sciences 2009; 10(9): 3722–3742. doi: 10.3390/ijms10093722
15. Kopinke FD, Mackenzie K. Mechanistic aspects of the thermal degradation of poly(lactic acid) and poly(β-hydroxybutyric acid). Journal of Analytical and Applied Pyrolysis 1997; 40–41: 43–53. doi: 10.1016/S0165-2370(97)00022-3
16. Lin Z, Guo X, He Z, et al. Thermal degradation kinetics study of molten polylactide based on Raman spectroscopy. Polymer Engineering & Science 2021; 61(1): 201–210. doi: 10.1002/pen.25568
17. Kalampounias AG, Kastrissios DT, Yannopoulos SN. Structure and vibrational modes of sulfur around the λ-transition and the glass-transition. Journal of Non-Crystalline Solids 2003; 326–327: 115–119. doi: 10.1016/S0022-3093(03)00388-0
18. Kalampounias AG, Kirillov SA, Steffen W, Yannopoulos SN. Raman spectra and microscopic dynamics of bulk and confined salol. Journal of Molecular Structure 2003; 651–653: 475–483. doi: 10.1016/S0022-2860(03)00128-5
19. Latsis GK, Banti CN, Kourkoumelis N, et al. Poly organotin acetates against DNA with possible implementation on human breast cancer. International Journal of Molecular Sciences 2018; 19(7): 2055. doi: 10.3390/ijms19072055
20. Wrona M, Cran MJ, Nerin C, Bigger SW. Development and characterisation of HPMC films containing PLA nanoparticles loaded with green tea extract for food packaging applications. Carbohydrate Polymers 2017; 156: 108–117. doi: 10.1016/j.carbpol.2016.08.094
21. Dharmalingam K, Anandalakshmi R. Fabrication, characterization and drug loading efficiency of citric acid crosslinked NaCMC-HPMC hydrogel films for wound healing drug delivery applications. International Journal of Biological Macromolecules 2019; 134: 815–829. doi: 10.1016/j.ijbiomac.2019.05.027
22. Jamshidi K, Hyon SH, Ikada Y. Thermal characterization of polylactides. Polymer 1988; 29(12): 2229–2234. doi: 10.1016/0032-3861(88)90116-4
23. Liu X, Zou Y, Li W, et al. Kinetics of thermo-oxidative and thermal degradation of poly(D,L-lactide) (PDLLA) at processing temperature. Polymer Degradation and Stability 2006; 91(12): 3259–3265. doi: 10.1016/j.polymdegradstab.2006.07.004
24. Acierno S, Van Puyvelde P. Rheological behavior of polyamide 11 with varying initial moisture content. Journal of Applied Polymer Science 2005; 97(2): 666–670. doi: 10.1002/app.21810